Two-photon bioimaging utilizing supercontinuum light generated by a high-peak-power picosecond semiconductor laser source

Hiroyuki Yokoyama
Tohoku University
New Industry Creation Hatchery Center (NICHe)
6-6-10 Aramaki-Aoba, Aoba-ku
Sendai 980-8579, Japan
E-mail: yoko@niche.tohoku.ac.jp

Hiroshi Tsubokawa
Tohoku University
Graduate School of Information Sciences
6-3-09 Aramaki-Aoba, Aoba-ku
Sendai 980-8579, Japan

Hengchang Guo
Tohoku University
New Industry Creation Hatchery Center (NICHe)
6-6-10 Aramaki-Aoba, Aoba-ku
Sendai 980-8579, Japan

Jun-ichi Shikata
Tohoku University
Research Institute of Electrical Communication (RIEC)
2-1-1 Katahira, Aoba-ku
Sendai 980-8577, Japan

Ki-ichi Sato
Keijiro Takashima
Tohoku University
New Industry Creation Hatchery Center (NICHe)
6-6-10 Aramaki-Aoba, Aoba-ku
Sendai 980-8579, Japan

Kaori Kashiwagi
Naoaki Saito
Kobe University
Biosignal Research Center
1-1 Rokkodai-cho, Nada-ku
Kobe 657-8501, Japan

Hirokazu Taniguchi
Hiromasa Ito
Tohoku University
Research Institute of Electrical Communication (RIEC)
2-1-1 Katahira, Aoba-ku
Sendai 980-8577, Japan

Abstract. We developed a novel scheme for two-photon fluorescence bioimaging. We generated supercontinuum (SC) light at wavelengths of 600 to 1200 nm with 774-nm light pulses from a compact turn-key semiconductor laser picosecond light pulse source that we developed. The supercontinuum light was sliced at around 1030- and 920-nm wavelengths and was amplified to kW-peak-power level using laboratory-made low-nonlinear-effects optical fiber amplifiers. We successfully demonstrated two-photon fluorescence bioimaging of mouse brain neurons containing green fluorescent protein (GFP).
 [DOI: 10.1117/1.2800393]

Keywords: semiconductor lasers; frequency conversion; ultrafast nonlinear optics; fluorescence microscopy; multiphoton processes; picosecond phenomena.

Paper 07186LRR received May 25, 2007; revised manuscript received Aug. 22, 2007; accepted for publication Aug. 23, 2007; published online Nov. 1, 2007.

Introduction

Supercontinuum (SC) light from visible wavelengths to the 1-μm region has attracted much attention as a novel physical phenomenon because it has become easy to generate using a nonlinear optical photonic crystal fiber (PCF) and a femtosecond pulse Ti-doped sapphire laser.[1–3] Previously, SC light has been utilized to control the absolute frequencies of optical combs[4,5] and tested for feasibility in high-speed optical com-

Tel: 81–22–795–4012; Fax: 81–22–795–4111; E-mail: yoko@niche.tohoku.ac.jp

1083-3668/2007/12(5)/054019/5/$25.00 © 2007 SPIE

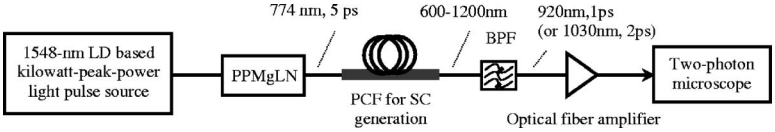

Fig. 1 Schematic configuration of supercontinuum (SC) light generation utilizing a gain-switched laser diode (LD)-based 1-kW-peak-power light pulse source. PPMgLN: periodically poled MgO-doped $LiNbO_3$; PCF: photonic crystal fiber; BPF: optical band pass filter.

munications in the 1.55-μm wavelength region.[6,7] Recently, SC light application has been extended to multiphoton bioimaging.[8,9] In general, however, for SC generation, the peak power of the light source should exceed 1 kW, and this requirement usually leads to the use of large and expensive mode-locked solid-state lasers. In this paper, we report a compact and stable configuration to generate SC light utilizing a semiconductor laser picosecond light pulse source.[10] Using amplified SC light pulses at appropriate wavelengths, successful two-photon fluorescence imaging (TPI) of mouse brain neurons containing green fluorescent protein (GFP) was demonstrated.

2 Methods

2.1 *SC Light Generation*

Figure 1 presents a schematic diagram of our SC light pulse source. SC light was generated by a PCF from incident 774-nm light pulses with 1-kW peak power and 5-ps duration. The 774-nm light pulses were the second-harmonic (SH) output of amplified 1548-nm gain-switching semiconductor laser diode (LD) pulses, and the details of this light pulse source are described in Ref. 10. For second-harmonic generation (SHG), we used a 5-mm-long bulk crystal of a periodically poled MgO-doped $LiNbO_3$ (PPMgLN) device. Previously, we reported the successful application of these SH light pulses with 1-kW peak power for TPI.[10] Here, we used these SH light pulses to generate stable SC light with a maximal bandwidth exceeding one octave. We have already described 300-nm-wide (1/4 octave) SC light generation,[11] and the great improvement reported here is due to an SH conversion efficiency increase to over 50% by further suppressing nonlinear optic spectral broadening inside the fiber amplifier for 1548-nm light pulses.[12]

The typical optical spectrum of the SC light generated is shown in Fig. 2. In this case, we injected 1-kW-peak-power SH pulses into a 50-m-long PCF that had a zero-dispersion wavelength near 800 nm.[11] Since the coupling efficiency of light pulses to the PCF was approximately 25%, the peak power of the light pulses inside the PCF was 250 W. At an intensity 10 dB lower than the peak, spectrum broadening exceeding one octave was observed. Although the short-wavelength region in Fig. 2 was limited to 600 nm because of the spectrometer measurement spectral region, we also confirmed violet light components in a prism-resolved spectral measurement.

2.2 *Optical Filtering and Amplification*

For the TPI application, we extracted infrared light components using an approximately 10-nm-wide full width at half maximum optical filter because the average optical power must be kept above a few tens of microwatts to amplify the filtered SC light to a power sufficient for TPI using optical fiber amplifiers. Fortunately, the spectral purity of the excitation light pulses is not an important requirement in TPI, which means that it is not necessary to generate Fourier-transform-limited light pulses. Indeed, the measured pulse width was 2 ps, which is the same value as that obtained with a 2-nm-wide optical bandpass filter. For 1030-nm light amplification, a laboratory-made Yb-doped fiber amplifier (YDFA) that consisted of a preamplifier and a main amplifier was used, in which the active fiber length was approximately 4 m. Except for the Yb-doped gain fibers, all of the optical couplings were built using free-space optics geometry to dispense with coupling fibers in order to avoid the nonlinear optical effects induced in these fibers. The measured maximum output power from the 1030-nm YDFA was approximately 100 mW with excitation from a 980-nm LD. The light pulse was broadened to 7-ps duration by fiber dispersion. Based on careful measurement, we found that approximately 20% of the light power accumulated between light pulses as amplified spontaneous emission (ASE) at a 10-MHz repetition frequency.

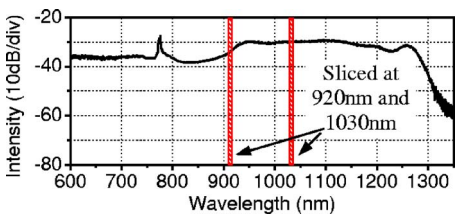

Fig. 2 A typical optical spectrum for supercontinuum light generated from a 50-m-long photonic crystal fiber. Dotted lines indicate the sliced-out wavelengths around 920 and 1030 nm.

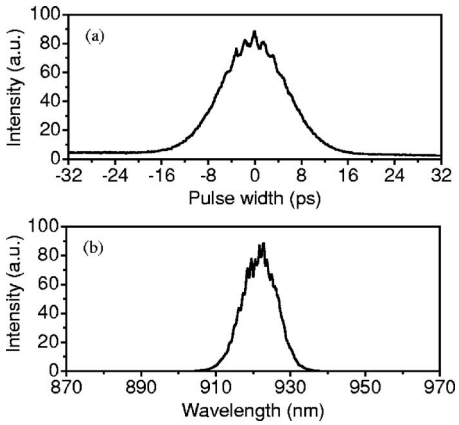

Fig. 3 (a) Second-harmonic generation (SHG) intensity autocorrelation trace for 920-nm light pulses indicating an 8-ps duration ($sech^2$ shape assumed), and (b) the corresponding optical spectrum.

Therefore, when the pulse repetition rate was 10 MHz, the peak power of the 7-ps light pulse was estimated to be 1.1 kW at average light power of 100 mW.

A similar procedure was adopted for generating high-peak-power 920-nm light pulses. In this case, 1-ps, 920-nm SC light pulses were amplified with a custom-made Nd-doped fiber amplifier (NDFA) pumped by an 810-nm LD. Since the active fiber in this NDFA was up to 16 m long, the light pulse was broadened to 8 ps at the end of the NDFA because of fiber dispersion. Figures 3(a) and 3(b) show an SHG intensity autocorrelation trace and an optical spectrum for amplified 920-nm light pulses. Because we found that the ASE is more severe in the NDFA than in the YDFA, we increased the light pulse repetition rate to 50 MHz to reduce the influence of the ASE. At this repetition rate, the estimated ASE ratio was 50%, and the peak power of the light pulses was 250 W when the average output power was 200 mW.

2.3 *Advantages of Our Light Source*

Here, we should clarify some of the advantages of our light pulse source for TPI. Although kW-peak-power ps and fs optical pulses have been used in nonlinear multiphoton bioimaging (MPI), including two- or three-photon excitation fluorescence,[13,14] second- or third-harmonic generation (SHG, THG),[15,16] and coherent anti-Stokes Raman scattering (CARS),[17] TPI is the most widely used imaging technology. For TPI, mode-locked Ti:sapphire lasers (MLTLs) are generally used[14–17]; however, they are expensive and require a great deal of maintenance. Furthermore, the tunable wavelength range of conventional MLTLs is between 700 and 900 nm. Although we demonstrated a TPI with a stable turn-key 774-nm light pulse source, as shown in Fig. 1,[10] a drawback of this light pulse source was that the wavelength was fixed at an SHG of 1548 nm. Therefore, we tried to expand the light pulse wavelength so that it was widely selectable by generating SC light. In our light pulse source scheme, necessary spectral components can be extracted, and control of the power level of an optical fiber amplifier can increase the light power to the level necessary for TPI. Note that the maximal LD light power used in our scheme is still limited to a few 100 mW, and this low average-power feature will allow a compact light source once we establish the entire design. Furthermore, the light pulses are synchronized to the electronic pulses driving the LD, so the repetition rate is flexibly variable simply by changing the electronic pulse frequency. This feature is useful for obtaining the best quality of TPI pictures, as demonstrated in Ref. 10.

3 Results

For TPI, amplified SC light pulses are directed into a two-photon fluorescence microscope that has been modified with a pair of galvanometer mirrors and a step motor for a three-dimensional (3-D) scanning system.[10] Last, the laser beam is focused by a 60× (1.2 NA) water-immersion objective onto a biological sample. The optical transmission efficiency was measured to be at most 20% from the light source to the specimen surface in the 920- to 1030-nm wavelength region.

3.1 *TPI of Mouse Kidney Tissues Stained with Alexa Fluo 488*

To test the feasibility of our light pulse source, a section of mouse kidney stained with Alexa Fluor 488 (Molecular Probes F24630; Invitrogen, Carlsbad, California) was used as the TPI specimen. The clear high-resolution image of the distal convoluted tubules and collecting tubules in the renal medulla indicated that TPI was successful, using 1030-nm optical pulses from our SC light source. At a 10-MHz repetition rate, the average measured optical power used was 40 mW from YDFA, giving an approximately 5-mW average power (70-W peak power) on the sample surface considering the 20% ASE ratio.

3.2 *TPI of Mouse brain Neurons Containing GFP*

Next, we attempted to image fluorescent proteins in mouse brain neurons using TPI. Fluorescent proteins, such as green, yellow, and red fluorescent proteins (GFP, YFP, and RFP), are widely used to stain specific molecules in particular cell organelles both *in vivo* and *in vitro*.[18] We examined the fluorescence of GFP, which is genetically bound to intracellular protein kinase C (PKC).[19] Although PKC is a key enzyme that modulates the function of neurons in the brain,[20] little is known about the subcellular distribution of its activities. Since the two-photon absorption wavelength range of GFP is generally shorter than 1 μm, we tried using 920-nm light pulses.

Figure 4 shows the TPI of γ-type PKC in a mouse Purkinje neuron. At a 50-MHz repetition rate, 160-mW average power (200-W peak power) from the light source, and consequent average power of approximately 16 mW (20-W peak power) on the sample surface considering the 50% ASE ratio, we detected GFP signals from the cell body [Fig. 4(a)] and dendrites [Fig. 4(b)]. We found that γ-type PKC was uniformly distributed in the intracellular space around the cell body. By contrast, the GFP signal in the dendrite was not uniform and was localized as bright spots on the branch. Dendrites are the primary locus of synaptic inputs and their integration, which are responsible for the activities of various ion channels, pumps, and transporters. Since these membrane-associated proteins are highly regulated by intracellular molecules, including PKC, the dendritic localization of the enzyme revealed using TPI suggests that γ-type PKC functions at its target proteins. These results clearly demonstrate that our SC light pulse source provides a useful wavelength region for the TPI of fluorescent proteins and redder dyes.

4 Conclusions

In summary, we carried out two-photon fluorescence bioimaging using amplified supercontinuum light pulses. Octave-wide SC light was generated using a compact stable semiconductor laser ps light pulse source and then filtered and amplified at wavelengths around 1030 and 920 nm. The 920-nm light pulses were effective for the two-photon excitation of GFP, while the 1030-nm light pulses were effective for YFP, RFP, and many other dyes. Note that our scheme is applicable to other light wavelengths within a generated SC bandwidth if we can create a proper optical amplifier. In practice, optical amplifiers are obtainable for wavelength regions of 980 and 1010 to 1120 nm with YDFAs[21,22]; 900 to 945,

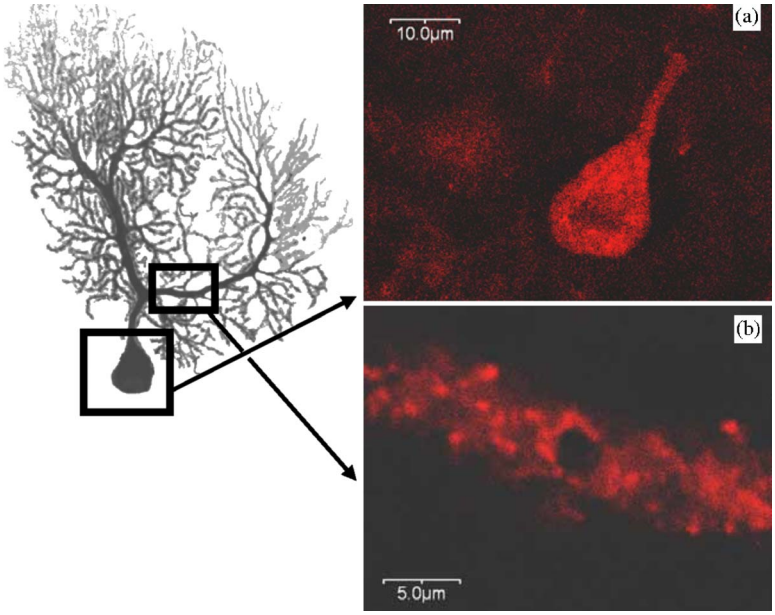

Fig. 4 Two-photon fluorescence images of the GFP bound to γ-type PKC in the soma (a) and dendrite (b) of a cerebellar Purkinje cell excited using amplified 920-nm light pulses at a 50-MHz repetition rate and 160-mW average power from the light source (16-mW average power and 20-W peak power on the sample surface considering the 50% ASE ratio). The shape of a Purkinje cell is shown schematically in the inset, and the regions for TPI are indicated by squares in the inset.

1070 to 1135, and 1310 to 1390 nm with NDFAs[23,24]; and 1260 to 1330 nm with Pr-doped fiber amplifiers (PDFAs).[25] Therefore, our light source will be applicable for many multiphoton bioimaging methods, including two- or three-photon fluorescence, SHG or THG, and CARS.

Acknowledgments

We are grateful to Central Glass and Sumitomo Osaka Cement for their support in developing the low-nonlinear-effect optical fiber amplifiers. This work was partly supported by the Japan Science and Technology Agency (JST), a Grant-in-Aid for Scientific Research (B) (No. 16360037) from the Japan Society for the Promotion of Science (JSPS), and a research grant from the Collaborative Research Program of the Center for Interdisciplinary Research at Tohoku University. H. C. Guo is supported by a JSPS Postdoctoral Fellowship.

References

1. J. Herrmann, U. Griebner, N. Zhavoronkov, A. Husakou, D. Nickel, J. C. Knight, W. J. Wadsworth, P. St. J. Russell, and G. Korn, "Experimental evidence for supercontinuum generation by fission of higher-order solitons in phonic fibers," *Phys. Rev. Lett.* **88**, 173901 (2002).
2. W. J. Wadsworth, J. C. Knight, A. Ortigosa-Blanch, J. Arriaga, E. Silvestre, and P. St. J. Russell, "Soliton effects in photonic crystal fibres at 850 nm," *Electron. Lett.* **36**, 53–55 (2000).
3. S. Coen, A. H. L. Chau, R. Leonhardt, J. D. Harvey, J. C. Knight, W. J. Wadsworth, and P. St. J. Russell, "Supercontinuum generation by stimulated Raman scattering and paprametric four-wave mixing in photonic crystal fibers," *J. Opt. Soc. Am. B* **19**, 753–764 (2002).
4. D. J. Jones, S. A. Diddams, J. K. Ranka, A. Stentz, R. S. Windeler, J. L. Hall, and S. T. Cundiff, "Carrier-envelope phase control of femtosecond mode-locked lasers and direct optical frequency synthesis," *Science* **288**, 635–639 (2000).
5. R. Holzwarth, Th. Udem, T. W. Hänsch, J. C. Knight, W. J. Wadsworth, and P. St. J. Russell, "Optical frequency synthesizer for precision spectroscopy," *Phys. Rev. Lett.* **85**, 2264–2267 (2000).
6. T. Morioka, S. Kawanishi, K. Mori, and M. Saruwatari, "Transform-limited, femtosecond WDM pulse generation by spectral filtering of gigahertz supercontinuum," *Electron. Lett.* **30**, 1166–1167 (1994).
7. K. Mori, H. Takara, S. Kawanishi, M. Saruwatari, and T. Morioka, "Flatly broadened supercontinuum spectrum generated in a dispersion decreasing fibre with convex dispersion profile," *Electron. Lett.* **33**, 1806–1808 (1997).
8. H. N. Paulsen, K. M. Hilligse, J. Thgersen, S. R. Keiding, and J. J. Larsen, "Coherent anti-Stokes Raman scattering microscopy with a photonic crystal fiber based light source," *Opt. Lett.* **28**, 1123–1125 (2003).
9. K. Isobe, W. Watanabe, S. Matsunaga, T. Higashi, K. Fukui, and K. Itoh, "Multi-spectral two-photon excited fluorescence microscopy using supercontinuum light source," *Jpn. J. Appl. Phys.* **44**, L167–169 (2005).
10. H. Yokoyama, H. C. Guo, T. Yoda, K. Takashima, K. Sato, H. Taniguchi, and H. Ito, "Two-photon bioimaging with picosecond optical pulses from a semiconductor laser," *Opt. Express* **14**, 3467–3471 (2006).
11. T. Yoda, H. Yokoyama, K. Sato, H. Taniguchi, and H. Ito, "High-peak-power picosecond optical-pulse generation with a gain-switched semiconductor laser, and high-efficiency wavelength conversion," in *Pacific Rim Conference on Lasers and Electro-Optics (CLEO-PR)*, CFM2-5, Tokyo (2005).
12. Y. Kubota, T. Teshima, N. Nishimura, S. Kanto, S. Sakaguchi, Z. Meng, Y. Nakata, and T. Okada, "Novel Er and Ce codoped fluoride fiber amplifier for low-noise and high-efficient operation with 980-nm pumping," *IEEE Photon. Technol. Lett.* **15**, 525–527 (2003).
13. W. Denk, J. H. Strickler, and W. W. Web, "Two-photon excitation in laser scanning microscopy," *Science* **248**, 73–76 (1990).
14. S. Maiti, J. B. Shear, R. M. Williams, W. R. Zipfel, and W. W. Webb, "Measuring serotonin distribution in living cells with three-photon excitation," *Science* **275**, 530–532 (1997).
15. R. Gauderon, P. B. Lukins, and C. J. R. Sheppard, "Three-dimensional second-harmonic generation imaging with femtosecond laser pulses," *Opt. Lett.* **23**, 1209–1211 (1998).
16. Y. Barad, H. Eisenberg, M. Horowitz, and Y. Silberberg, "Nonlinear scanning laser microscopy by third harmonic generation," *Appl. Phys. Lett.* **70**, 922–924 (1997).
17. A. Zumbush, G. R. Holtom, and X. S. Xie, "Three-dimensional vibrational imaging by coherent anti-Stokes Raman scattering," *Phys. Rev. Lett.* **82**, 4142–4145 (1999).

18. W. R. Zipfel, R. M. Williams, and W. W. Webb, "Nonlinear magic: multiphoton microscopy in the biosciences," *Nat. Biotechnol.* **21**, 1369–1377 (2003).
19. N. Sakai, H. Tsubokawa, M. Matsuzaki, T. Kajimoto, E. Takahashi, Y. Ren, S. Ohmori, Y. Shirai, H. Matsubayashi, J. S. Chen, R. S. Duman, H. Kasai, and N. Saito, "Propagation of γPKC translocation along the dendrites of Purkinje cell in γPKC-GFP transgenic mice," *Genes Cells* **9**, 945–957 (2004).
20. C. Tanaka and Y. Nishizuka, "The protein kinase C family for neuronal signaling," *Annu. Rev. Neurosci.* **17**, 551–567 (1994).
21. K. Taira, T. Hashimoto, and H. Yokoyama, "Two-photon fluorescence imaging with a pulse source based on a 980-nm gain-switched laser diode," *Opt. Express* **15**, 2454–2458 (2007).
22. J. Nilsson, W. A. Clarkson, R. Selvas, J. K. Sahu, P. W. Turner, S.-U. Alam, and A. B. Grudonon, "High-power wavelength-tunable cladding-pumped rare-earth-doped silica fiber lasers," *Opt. Fiber Technol.* **10**, 5–30 (2004).
23. I. P. Alcock, A. I. Ferguson, D. C. Hanna, and A. C. Tropper, "Tunable, continuous-wave neodymium-doped monomode-fiber laser operating at 0.900–0.945 and 1.070–1.135 μm," *Opt. Lett.* **11**, 709–711 (1986).
24. B. N. Samson, P. A. Tick, and N. F. Borrelli, "Efficient neodymium-doped glass-ceramic fiber laser and amplifier," *Opt. Lett.* **26**, 145–147 (2001).
25. T. Whitley, R. Wyatt, D. Szebesta, and S. Davey, "High output power from an efficient praseodymium-doped fluoride fiber amplifier," *IEEE Photon. Technol. Lett.* **4**, 401–403 (1993).